

Solvent-induced crystal-facet effect of nickel-cobalt layered double hydroxide for highly efficient overall water splitting

Lingxing Zan^a, Hongling Zhang^a, Zhangwen Ye^a, Qingbo Wei^a, Hongliang Dong^d,

Shiwen Sun^a, Qiang Weng^f, Xin Bo^e, Huicong Xia^{b}, Yibing Li^c *, Feng Fu^a **

^a Key Laboratory of Chemical Reaction Engineering of Shaanxi Province; College of Chemistry & Chemical Engineering, Yan'an University, Yan'an 716000, China.

^b College of Materials Science and Engineering, Zhengzhou University, Zhengzhou 450001, China.

^c Institute of Smart City and Intelligent Transportation, Southwest Jiaotong University, Chengdu, 610097, China.

^d State Key Laboratory of High Performance Ceramics and Superfine Microstructure, Shanghai Institute of Ceramics, Chinese Academy of Sciences, Shanghai 201899, China.

^e School of Chemistry, University of New South Wales, Sydney, Australia, 2052.

^f Key Laboratory of Applied Surface and Colloid Chemistry (MOE), Shaanxi Key Laboratory for Advanced Energy Devices, Shaanxi Engineering Laboratory for Advanced Energy Technology, School of Materials Science and Engineering, Shaanxi Normal University, Xi'an, 710119, China.

E-mail: *Huicong Xia* (summer9209@126.com)

Yibing Li (yibing.li@sjtu.edu.cn)

Feng Fu (yadxfufeng@126.com)

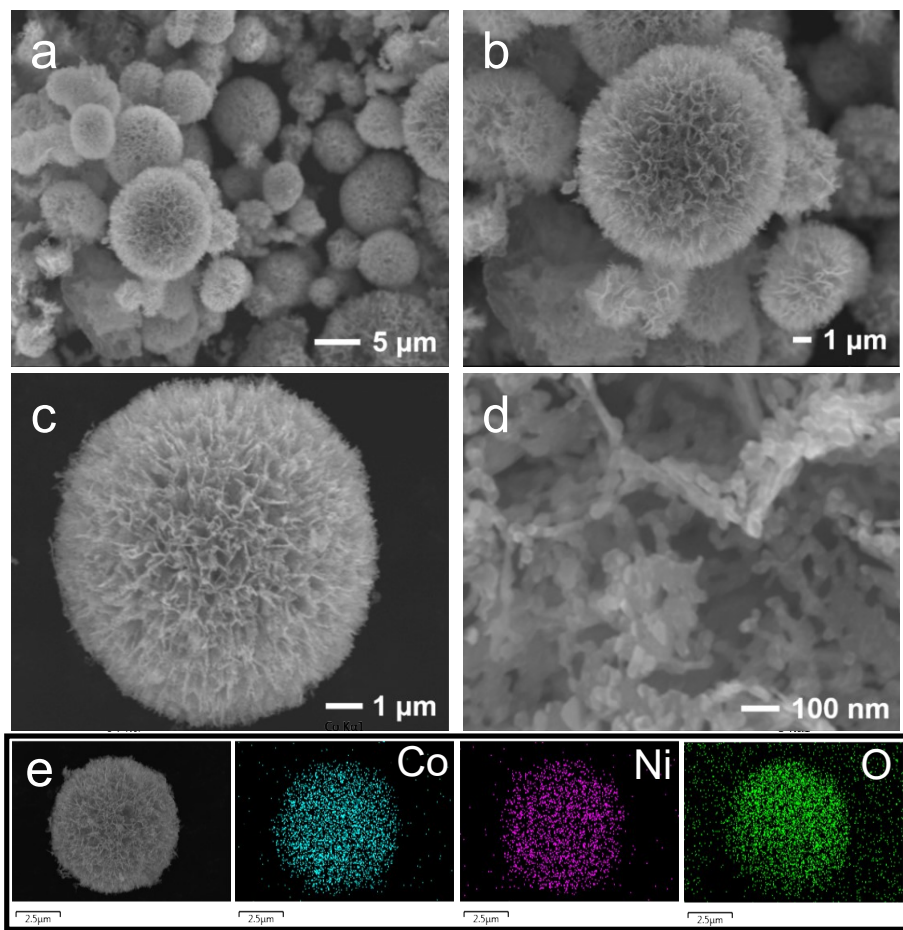


Fig. S1 Structural characterizations of $\text{Co}_{0.67}\text{Ni}_{0.33}(\text{OH})_2\text{-E}$. a-d, FESEM images. e, FESEM-EDS mapping images of Co, Ni and O elements.

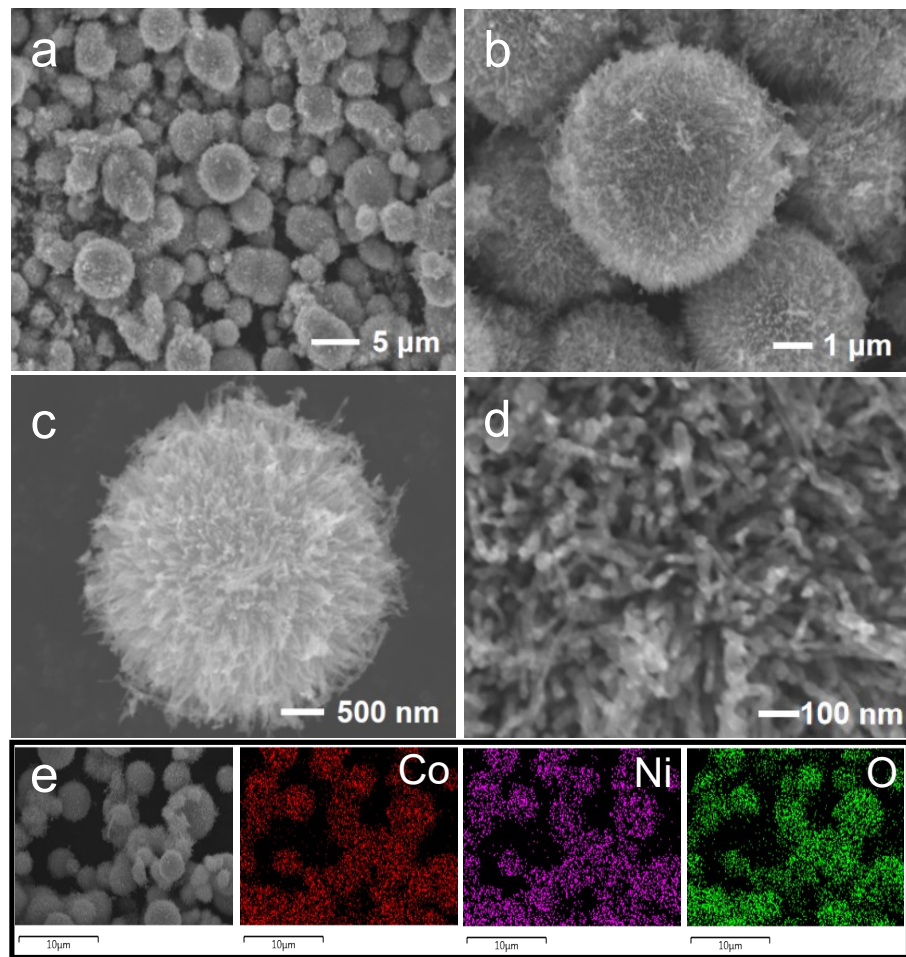


Fig. S2 Structural characterizations of $\text{Co}_{0.67}\text{Ni}_{0.33}(\text{OH})_2\text{-W}$. a-d, FESEM images. e, FESEM-EDS mapping images of Co, Ni and O elements.

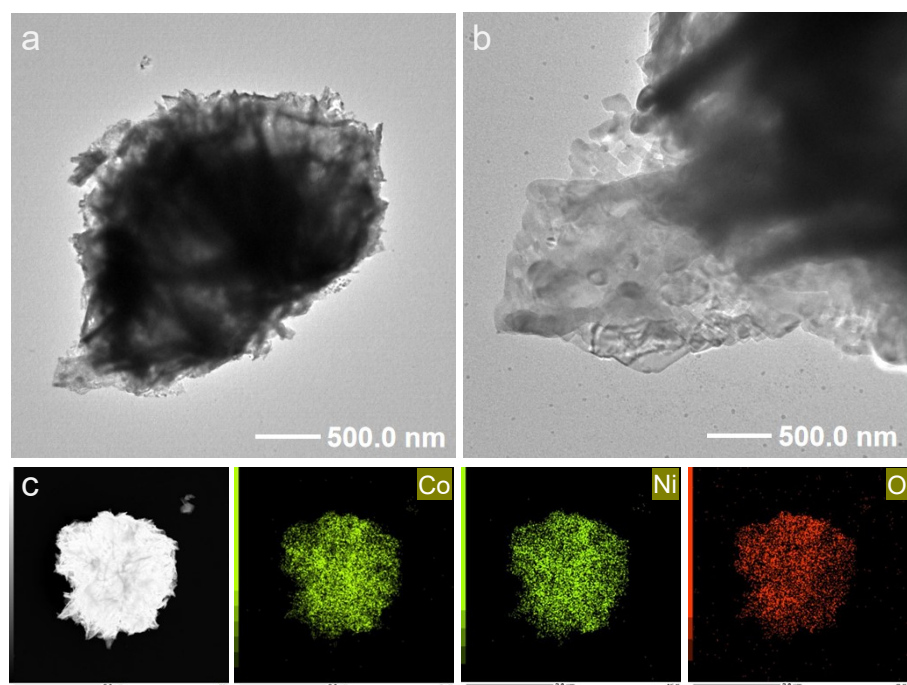


Fig. S3 Structural characterizations of $\text{Co}_{0.67}\text{Ni}_{0.33}(\text{OH})_2\text{-E}$. a-b, HRTEM images. c, HRTEM-EDX mapping images of Co, Ni and O elements.

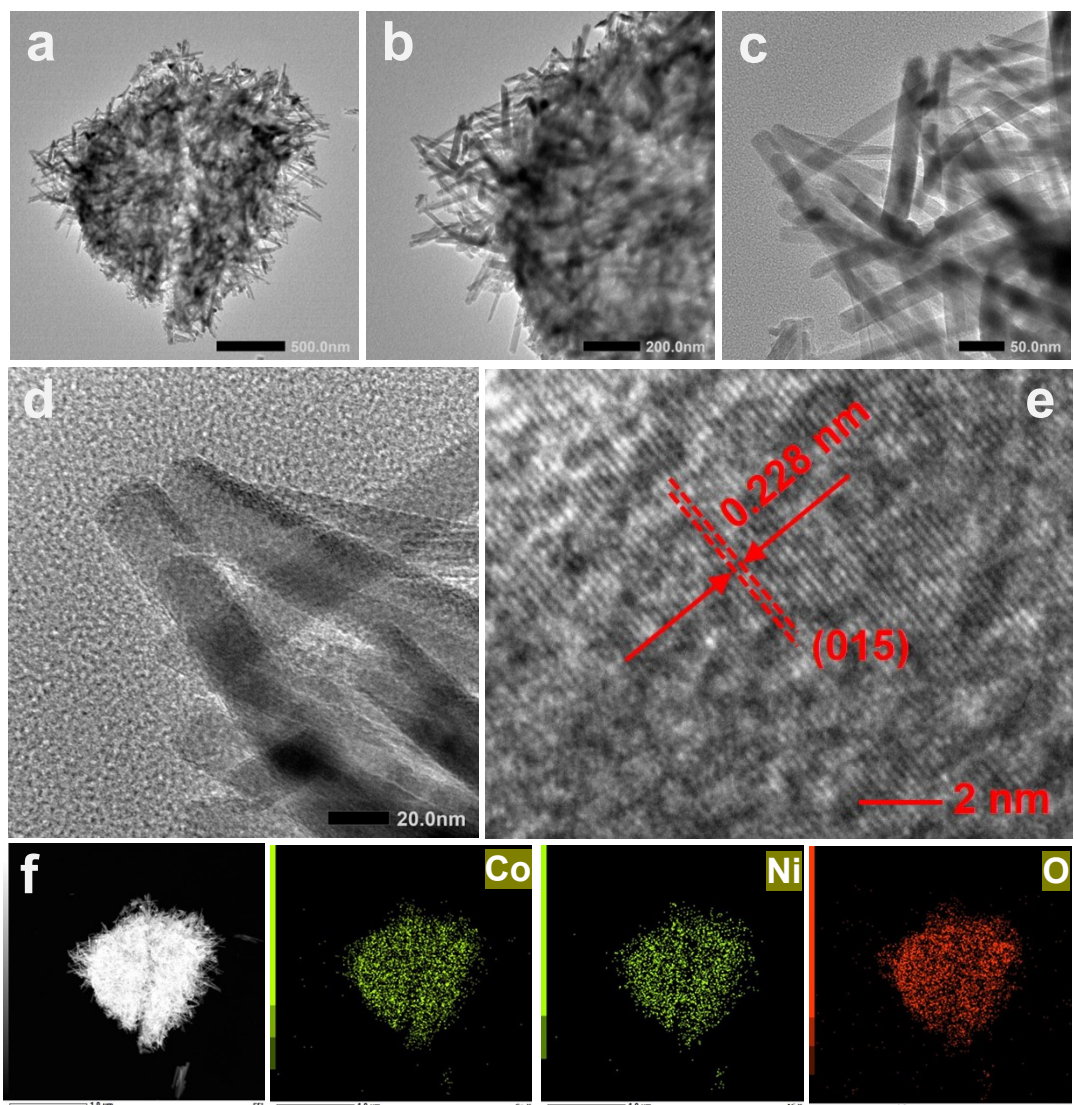


Fig. S4 Structural characterizations of $\text{Co}_{0.67}\text{Ni}_{0.33}(\text{OH})_2\text{-W}$. a-b, HRTEM images. c, HRTEM-EDX mapping images of Co, Ni and O elements.

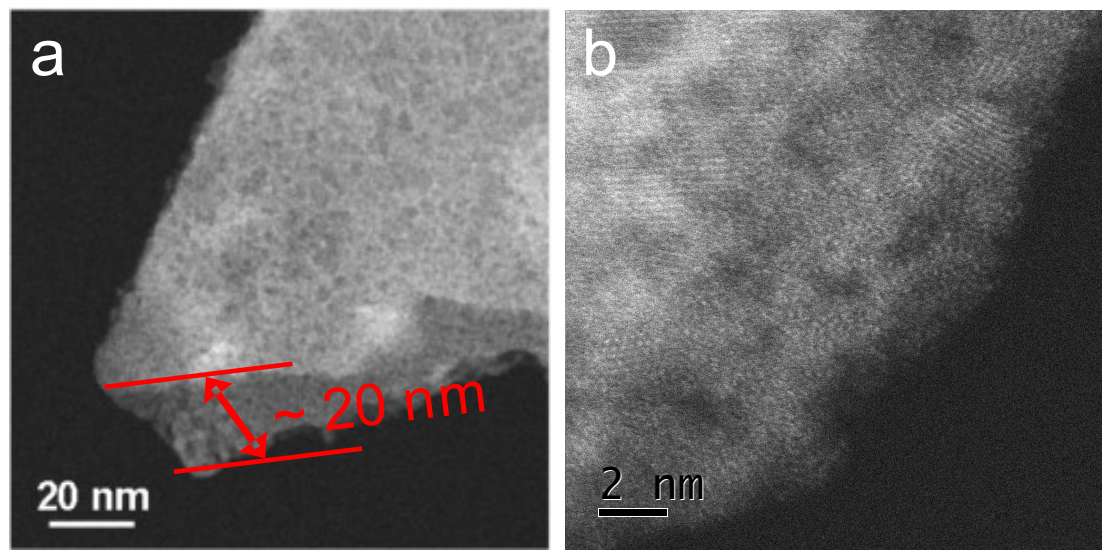


Fig. S5 Structural characterizations of $\text{Co}_{0.67}\text{Ni}_{0.33}(\text{OH})_2\text{-E}$.

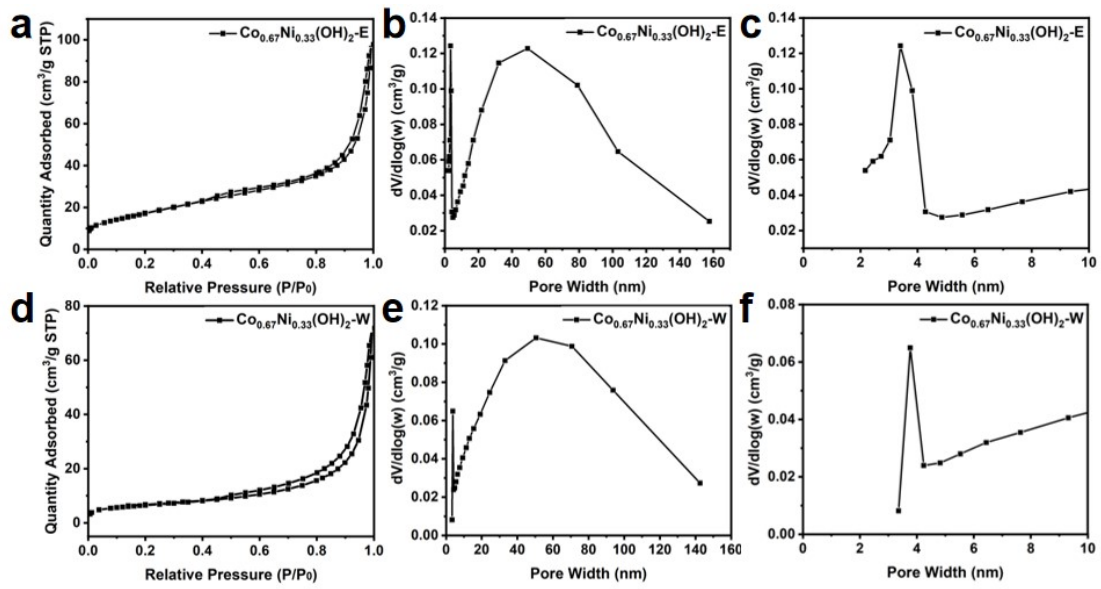


Fig. S6 Determination of the Brunauer-Emmett-Teller (BET) surface area. Nitrogen isothermal desorption curves for (a) $\text{Co}_{0.67}\text{Ni}_{0.33}(\text{OH})_2\text{-E}$ and (d) $\text{Co}_{0.67}\text{Ni}_{0.33}(\text{OH})_2\text{-W}$. Pore size distribution based on the BJH model for (b-c) $\text{Co}_{0.67}\text{Ni}_{0.33}(\text{OH})_2\text{-E}$ and (e-f) $\text{Co}_{0.67}\text{Ni}_{0.33}(\text{OH})_2\text{-W}$.

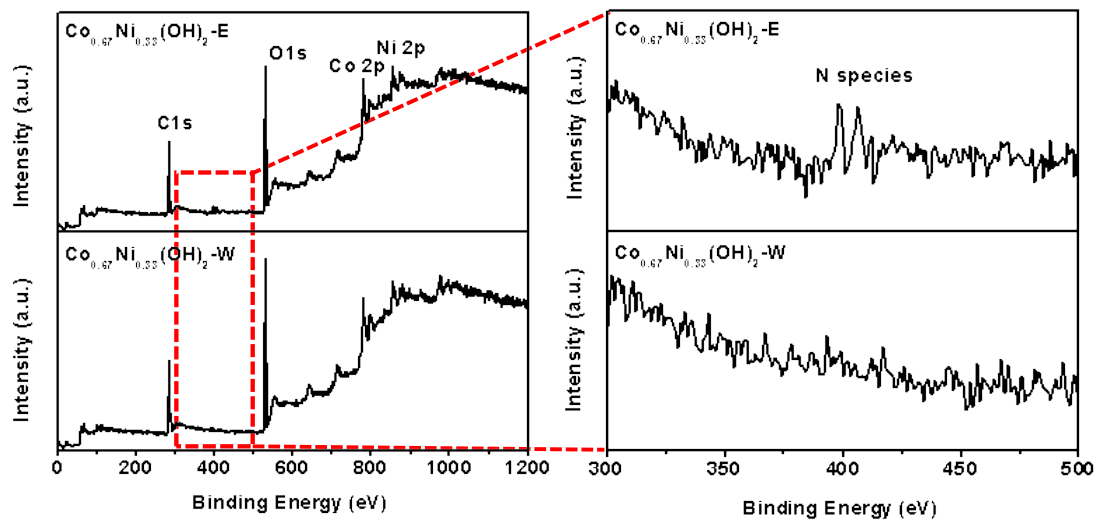


Fig. S7 High resolution XPS spectra. The survey spectra of $\text{Co}_{0.67}\text{Ni}_{0.33}(\text{OH})_2$ -E (up) and $\text{Co}_{0.67}\text{Ni}_{0.33}(\text{OH})_2$ -W (down).

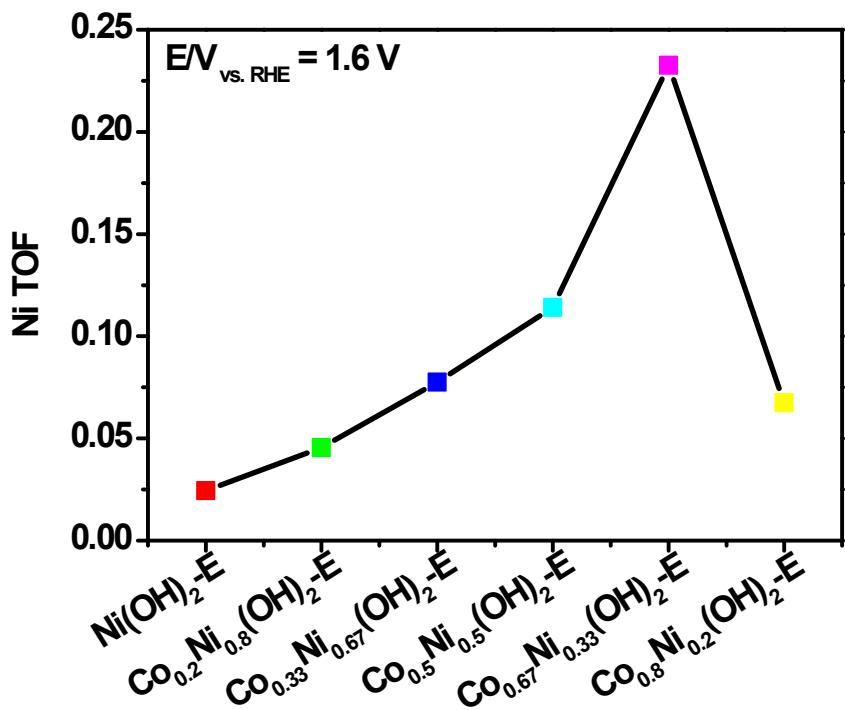


Fig. S8 Ni-TOF values of $\text{Co}_x\text{Ni}_{1-x}(\text{OH})_2\text{-E}$ at 1.6 V.

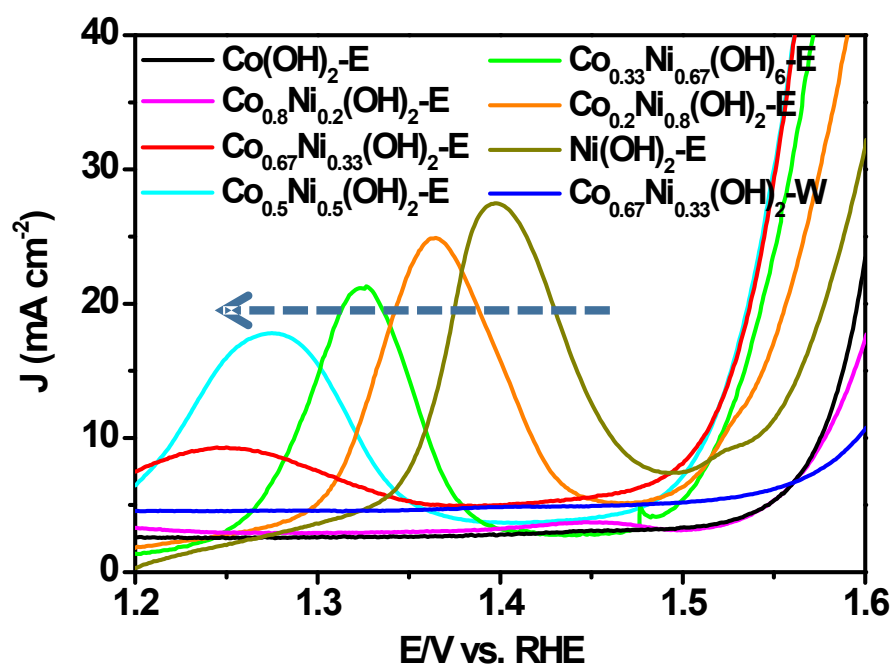


Fig. S9 Cyclic voltammograms of $\text{Co}_x\text{Ni}_{1-x}(\text{OH})_2$ surface in Ar-saturated 1 M KOH solution at a scan rate of 5 mV s^{-1} .

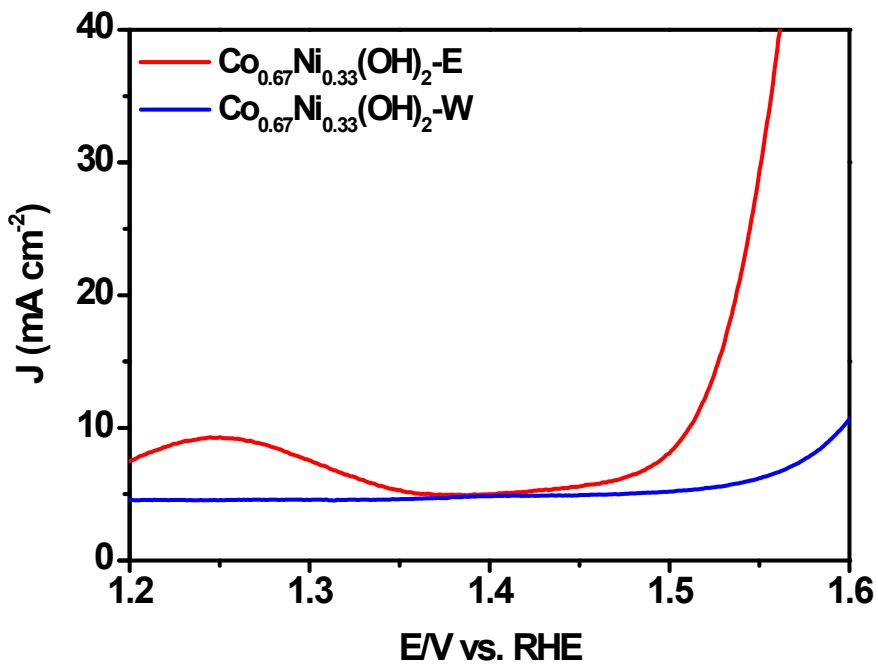


Fig. S10 Cyclic voltammograms of OER at $\text{Co}_x\text{Ni}_{1-x}(\text{OH})_2\text{-E}$ and $\text{Co}_x\text{Ni}_{1-x}(\text{OH})_2\text{-W}$ surface in Ar-saturated 1 M KOH solution at a scan rate of 5 mV s⁻¹.

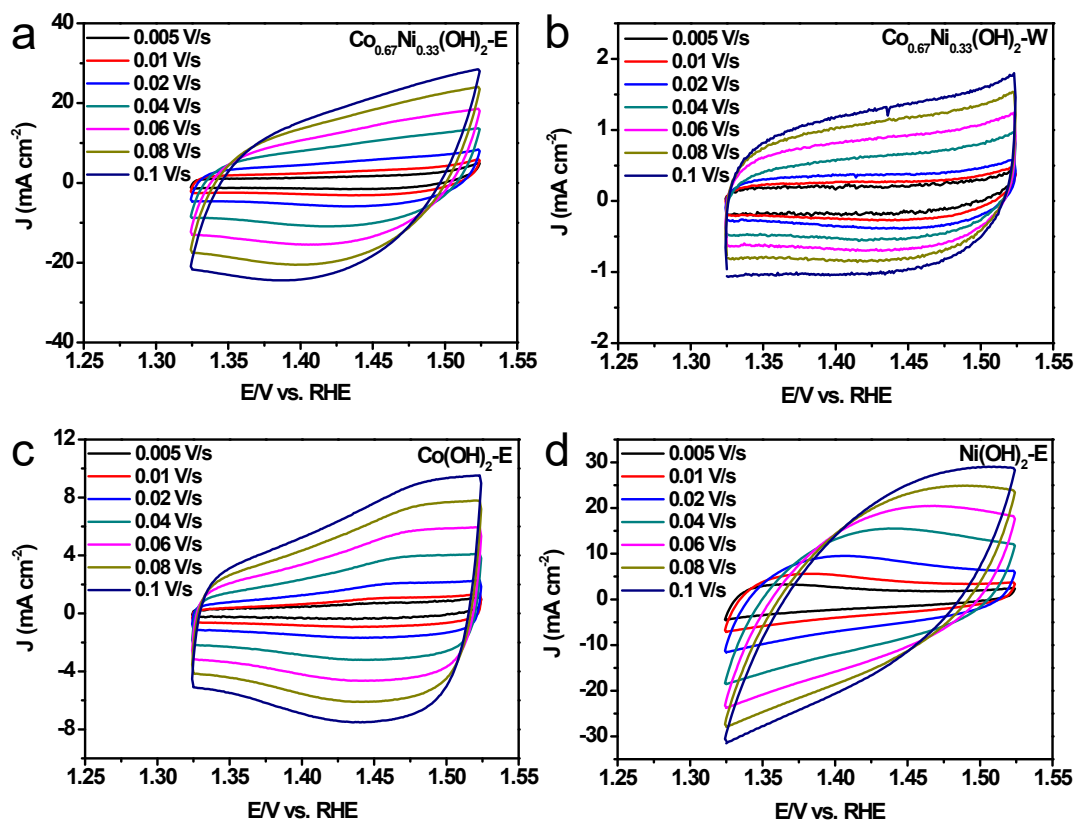


Fig. S11 Cyclic voltammograms of $\text{Co}_x\text{Ni}_{1-x}(\text{OH})_2$ surface in Ar-saturated 1 M KOH solution at a scan rate of 5 mV s^{-1} in the potential range of 1.325–1.525 V (vs. RHE). a, $\text{Co}_{0.67}\text{Ni}_{0.33}(\text{OH})_2\text{-E}$. b, $\text{Co}_{0.67}\text{Ni}_{0.33}(\text{OH})_2\text{-W}$. c, $\text{Co}(\text{OH})_2\text{-E}$. d, $\text{Ni}(\text{OH})_2\text{-E}$.

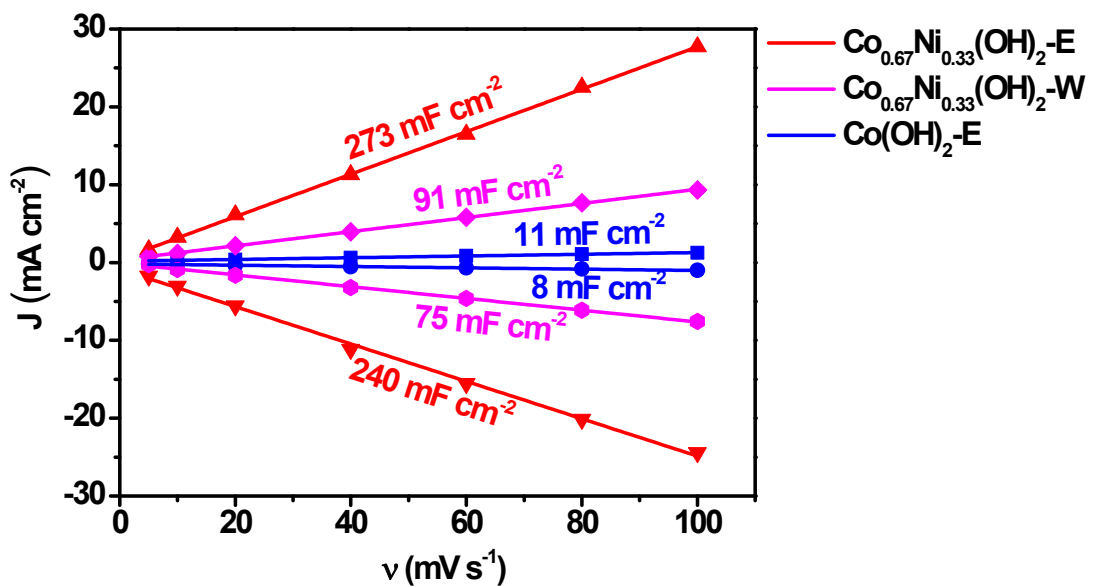


Fig. S12 The plots of scan rates vs. current densities corresponding to the cyclic voltammograms as shown in Fig. S11.

Table S1. Comparison of the OER performances of various (Ni or Co)-based LDH catalysts and noble metal catalysts.

Catalysts	Electrolyte	Substrate	Overpotential [mV] at specific current density	Tafel slope [mV dec ⁻¹]	Ref.
Exfoliated NiFe LDH	1 M KOH	GC	302@10 mA cm ⁻²	40	1
NiO/NiCo ₂ O ₄	1 M KOH	GC	357@10 mA cm ⁻²	130	2
NiCo ₂ P _x /CNTs	1 M KOH	GC	284@10 mA cm ⁻²	50.3	3
NiFe LDH/NiFe phosphate	1 M KOH	Carbon fiber paper	290@10 mA cm ⁻²	38	4
FeNi LDH/Ti ₃ C ₂ -MXene	1 M KOH	GC	298@10 mA cm ⁻²	43	5
CoNi LDH/CoO	1 M KOH	GC	300@10 mA cm ⁻²	123	6
NiCo ₂ O ₄ /NiCoFe LDH	1 M KOH	Carbon cloth	302@50 mA cm ⁻²	71.5	7
Ni _{0.6} Co _{1.4} P nanocages	1 M KOH	GC	300@10 mA cm ⁻²	80	8
CoNi/NC-YS	1 M KOH	Carbon fiber paper	292@10 mA cm ⁻²	53.8	9
CoNi-Fe ₃ N	1 M KOH	Iron foil	285@10 mA cm ⁻²	34	10
Ni _{0.75} Fe _{0.25} -LDH	1 M KOH	GC	~300@10 mA cm ⁻²	~50	11
NiCo-LDH nanosheets	1 M KOH	GC	~350@10 mA cm ⁻²	41	1
NiCo LDH nanoplates	1 M KOH	Carbon paper	367@10 mA cm ⁻²	40	12
Co _{1.8} Ni(OH) _{5.6} @Co _{1.8} NiS _{0.4} (OH) _{4.8}	0.1 M KOH	GC	274@10 mA cm ⁻²	45	13
IrO ₂ @SL-NiFe LDHs	1 M KOH	GC	270@10 mA cm ⁻²	59	14
SL-NiFe LDHs	1 M KOH	GC	343@10 mA cm ⁻²	139	14
IrO ₂	1 M KOH	GC	325@10 mA cm ⁻²	45	1
RuO ₂	1 M KOH	GC	291@10 mA cm ⁻²	81	15
Co _{0.67} Ni _{0.33} (OH) ₂ -E	1 M KOH	GC	280@10 mA cm ⁻²	81	This work

References

1. F. Song and X. Hu, Exfoliation of layered double hydroxides for enhanced oxygen evolution catalysis, *Nat. Commun.*, 2014, **5**, 4477.
2. Z. Zhang, X. Liang, J. Li, J. Qian, Y. Liu, S. Yang, Y. Wang, D. Gao and D. Xue, Interfacial engineering of NiO/NiCo₂O₄ porous nanofibers as efficient bifunctional catalysts for rechargeable zinc-air batteries, *ACS Appl. Mater. Interfaces*, 2020, **12**, 21661-21669.
3. C. Huang, T. Ouyang, Y. Zou, N. Li and Z.-Q. Liu, Ultrathin NiCo₂P_x nanosheets strongly coupled with CNTs as efficient and robust electrocatalysts for overall water splitting, *J. Mater. Chem. A*, 2018, **6**, 7420-7427.
4. Y. Li and C. Zhao, Enhancing water oxidation catalysis on a synergistic phosphorylated NiFe hydroxide by adjusting catalyst wettability, *ACS Catal.*, 2017, **7**, 2535-2541.
5. M. Yu, S. Zhou, Z. Wang, J. Zhao and J. Qiu, Boosting electrocatalytic oxygen evolution by synergistically coupling layered double hydroxide with MXene, *Nano Energy*, 2018, **44**, 181-190.
6. J. Wu, Z. Ren, S. Du, L. Kong, B. Liu, W. Xi, J. Zhu and H. Fu, A highly active oxygen evolution electrocatalyst: ultrathin CoNi double hydroxide/CoO nanosheets synthesized via interface-directed assembly, *Nano Res.*, 2016, **9**, 713-725.
7. Y. Liu, Y. Bai, Y. Han, Z. Yu, S. Zhang, G. Wang, J. Wei, Q. Wu and K. Sun, Self-supported hierarchical FeCoNi-LTH/NiCo₂O₄/CC electrodes with enhanced bifunctional performance for efficient overall water splitting, *ACS Appl. Mater. Interfaces*, 2017, **9**, 36917-36926.
8. B. Qiu, L. Cai, Y. Wang, Z. Lin, Y. Zuo, M. Wang and Y. Chai, Fabrication of nickel-cobalt bimetal phosphide nanocages for enhanced oxygen evolution catalysis, *Adv. Funct. Mater.*, 2018, **28**, 1706008.
9. G. Hou, X. Jia, H. Kang, X. Qiao, Y. Liu, Y. Li, X. Wu and W. Qin, CoNi nano-alloys modified yolk-shell structure carbon cage via *Saccharomyces* as carbon template for efficient oxygen evolution reaction, *Appl. Catal., B*, 2022,

315, 121551.

10. J. Dong, Y. Lu, X. Tian, F.-Q. Zhang, S. Chen, W. Yan, H.-L. He, Y. Wang, Y.-B. Zhang, Y. Qin, M. Sui, X.-M. Zhang and X. Fan, Genuine active species generated from Fe₃N nanotube by synergistic CoNi doping for boosted oxygen evolution catalysis, *Small*, 2020, **16**, 2003824.
11. K. Fan, H. Chen, Y. Ji, H. Huang, P. M. Claesson, Q. Daniel, B. Philippe, H. Rensmo, F. Li, Y. Luo and L. Sun, Nickel-vanadium monolayer double hydroxide for efficient electrochemical water oxidation, *Nat. Commun.*, 2016, **7**, 11981.
12. H. Liang, F. Meng, M. Cabán-Acevedo, L. Li, A. Forticaux, L. Xiu, Z. Wang and S. Jin, Hydrothermal continuous flow synthesis and exfoliation of NiCo layered double hydroxide nanosheets for enhanced oxygen evolution catalysis, *Nano Lett.*, 2015, **15**, 1421-1427.
13. B. Wang, C. Tang, H.-F. Wang, X. Chen, R. Cao and Q. Zhang, A nanosized CoNi hydroxide@Hydroxysulfide core-shell heterostructure for enhanced oxygen evolution, *Adv. Mater.*, 2019, **31**, 1805658.
14. D. Li, T. Li, G. Hao, W. Guo, S. Chen, G. Liu, J. Li and Q. Zhao, IrO₂ nanoparticle-decorated single-layer NiFe LDHs nanosheets with oxygen vacancies for the oxygen evolution reaction, *Chem. Eng. J.*, 2020, **399**, 125738.
15. J. Li, L. Wang, H. He, Y. Chen, Z. Gao, N. Ma, B. Wang, L. Zheng, R. Li, Y. Wei, J. Xu, Y. Xu, B. Cheng, Z. Yin and D. Ma, Interface construction of NiCo LDH/NiCoS based on the 2D ultrathin nanosheet towards oxygen evolution reaction, *Nano Res.*, 2022, **15**, 4986-4995.